*Research Article*

# Synthesis and Optical Properties of Au-Ag Alloy Nanoclusters with Controlled Composition

**J. F. Sánchez-Ramírez,[1, 2] U. Pal,[3] L. Nolasco-Hernández,[1] J. Mendoza-Álvarez,[2] and J. A. Pescador-Rojas[1]**

[1] *(CICATA-IPN), Legaría 694, Col. Irrigación, 11500 Mexico City, DF, Mexico*

[2] *Departamento de Física, Centro de Investigación y de Estudios Avanzados del IPN, Apartado Postal 14-740, 07000 Mexico City, DF, Mexico*

[3] *Instituto de Fisica, Universidad Autónoma de Puebla, Apartado Postal 48, 72570 Puebla, Mexico*

Correspondence should be addressed to U. Pal, upal@sirio.ifuap.buap.mx

Colloidal solid-solution-like Au-Ag alloy nanoclusters of different compositions were synthesized through citrate reduction of mixed metal ions of low concentrations, without using any other protective or capping agents. Optical absorption of the alloy nanoclusters was studied both theoretically and experimentally. The position of the surface plasmon resonance (SPR) absorption band of the nanoclusters could be tuned from 419 nm to 521 nm through the variation of their composition. Considering effective dielectric constant of the alloy, optical absorption spectra for the nanoclusters were calculated using Mie theory, and compared with the experimentally obtained spectra. Theoretically obtained optical spectra well resembled the experimental spectra when the true size distribution of the nanoparticles was considered. High-resolution transmission electron microscopy (HREM), high-angle annular dark field (HAADF) imaging, and energy dispersive spectroscopy (EDS) revealed the true alloy nature of the nanoparticles with nominal composition being preserved. The synthesis technique can be extended to other bimetallic alloy nanoclusters containing Ag.

## 1. INTRODUCTION

Recently, muchattention has been paid to the synthesis and characterizationof bimetallic nanoparticles due to their unique catalytic, electronic,optical, structural, and thermal-properties [1–5] and subsequent technological applications as catalysts, sensors, nanoelectronic devices [6–13], and biosensors [14]. The properties and hence the applicability of these nanoparticles not only depend on their size and shape, but also on the combination of the component metals (composition) and their fine structure, either as alloy or core-shell structures. Bimetallic nanoparticles particularly with well-defined alloy structures of noble metals like Pt-Ru, Cu-Pd, Pt-Mo, Pt-W, Pt-Ni, and Au-Ag provide practical examples for the influence of metals' composition and their structures on their catalytic properties [15–19]. Au-Ag nanoparticles of alloy-type structure exhibit high catalytic activities for low-temperature CO oxidation [12, 18] and aerobic oxidation of alcohol [20].

On the other hand, Au-Ag bimetallic nanoparticles show different optical responses for alloy and core-shell configurations, even when they have the same Au and Ag contents. Au-Ag alloy nanoparticles show a single, composition-sensitive absorption band located at an intermediate position between pure Au and Ag nanoparticles' surface plasmon resonance (SPR) peaks, which results in amplification of light-induced processes (e.g., Raman scattering) undergone by molecules localized on their surfaces, giving rise to surface-enhanced Raman scattering [21]. Thus, the control of structural type and composition of bimetallic nanoparticlescomprised of Ag and Au have been a subject of considerable interest; the development of simple and versatile methods for controlling the composition and structure of Au-Ag nanoparticles is an important and challenging task.

Bimetallic Au-Ag nanoparticles have been obtained using different synthesis methods including replacement reaction [22], biosynthesis [23], green synthesis [24], laser-assisted [25], alcohol reduction [26], borohydride reduction [27],

laser ablation [28], ultrasound irradiation [29], and metal evaporation-condensation methods [30]. However, relatively few methods produce true alloy nanoparticles due to phase separation at the atomic level leading to the formation of core-shell particles [31–35].

We have succeeded in synthesizing true Au-Ag alloy nanoparticles of varying Au/Ag molar ratios in water, by slightly modifying the citrate reduction method used by Link et al. [36]. Optical and structural properties of the samples were studied using optical absorption spectroscopy in the UV-Vis range, transmission electron microscopy (TEM), high-resolution TEM (HREM), and high-angle annular dark field (HAADF) imaging techniques. Considering effective dielectric constant of the alloy, optical absorption spectra for the nanoclusters were calculated using Mie theory, and compared with the experimentally obtained spectra.

## 2. EXPERIMENTAL AND THEORETICAL CALCULATIONS

### 2.1. Synthesis

Colloidal dispersions of bimetallic Au-Ag nanoparticles of different molar ratios were synthesized with a slight modification of conventional citrate reduction method without using any organic stabilizer. Typically, the method of citrate reduction involves concentrated solutions of metallic salts like $HAuCl_{4(s)}$ and $AgNO_{3(s)}$ and their simultaneous reduction with sodium citrate. However, the presence of high-concentration $Cl^-$ ions produced from the reduction of $HAuCl_4$ does not permit a complete dissolution of silver salts, hence reduction of $Ag^+$ ions due to spontaneous formation of $AgCl_{(s)}$. Considering the solubility product ($K_{ps}$) of $AgCl_{(s)}$ ($1.8 \times 10^{-10}$), to produce complete solubility of $AgNO_3$, it is necessary to use its solutions of concentrations lower than the ($K_{ps}$) of $AgCl_{(s)}$ [37]. To verify this criterion, we prepared two sets of metal ion solutions with different concentrations. In the first set, gold and silver ion solutions of 1.32 mM concentrations were prepared by dissolving $HAuCl_{4(s)}$ and $AgNO_{3(s)}$ in water, respectively. In the second set, metal ion solutions of $1.32 \times 10^{-3}$ mM were prepared in a similar way. Both solutions were mixed at room temperature at various Au/Ag molar ratios (= 9/1, 3/1, 1/1, 3/1, 1/9) to make a total volume of 25 mL of bimetallic ion mixture. While for the first batch of ionic solutions the solubility product was above the solubility product ($K_{ps}$) of $AgCl_{(s)}$, in the latter batch, the solubility product was below the ($K_{ps}$) of $AgCl_{(s)}$. To reduce the metal ions, 1 mL aqueous solution of sodium citrate ($3.5 \times 10^{-5}$ m mol in 5 mL of $H_2O$) was added to the mixture solutions at 100°C temperature under magnetic agitation, and refluxed for 1 hour. The same procedure was followed to prepare the monometallic Au and Ag colloids. Homogeneous colloidal dispersions were formed after the addition of reductor in the metal ion solutions. On adding the reductor, the color of the $HAuCl_4$ solution changed from clear yellow to red. In contrast, the $AgNO_3$ solution changed from colorless to light yellow. The intermediate compositions resulted in colors that are varying between yellow and red. While the colloidal solutions prepared with the first batch of solutions (with high metal ion concentrations) did precipitate after a couple of days, we did not observe any flocculation or precipitation for the second batch of samples (prepared with very low concentration of metal ions) even after a couple of months.

### 2.2. Characterizations

Room-temperature optical absorption spectra of the colloidal samples were recorded using a 10 mm path length quartz cuvette in a UV-Vis-NIR scanning spectrophotometer (Shimadzu UV 3101PC double beam). For transmission electron microscopic (TEM) observations, a drop of colloidal solution was spread on a carbon-coated copper microgrid and dried in vacuum. For electron microscopy analysis, two microscopes, a Jeol JEM200 and a Tecnai 200 TEM with field-emission gun by FEI, were used for the low-magnification and high-resolution observations of the samples, respectively. High-resolution electron microscope (HREM) images were digitally processed by using filters in the Fourier space. HAADF images were recorded with a Jeol 2010F microscope in the STEM mode, using a dark field detector. Energy dispersive spectroscopy of the samples was performed using a Jeol JSM6390 scanning electron microscope with NORAN analytical system attached.

### 2.3. Theoretical calculations

Formal solutions of the phenomena of light absorption and scattering by small metal particles are obtained using Mie theory [38–40]. The physical effect of light absorption by the metallic nanoparticles suspended in liquids is the coherent oscillation of conduction band electrons (SPR) through the interaction with electromagnetic filed, where the electronic transitions between the associated discrete energies give the extinction (absorption + diffusion) of a part of incident light resulting in a coloring effect in these systems. The absorption and dispersion of light in nanoparticles depend on the nature of the metals, along with their chemical composition, morphology, and sizes. In the case of spherical nanoparticles separated by long distance, with no substance adsorbed on their surfaces, their absorbance ($A$) can be calculated as

$$A = lC_{\text{ext}} \frac{C_{\text{Au}_x\text{Ag}_{x-1}}}{fr^3}, \tag{1}$$

where $r$ is the particle radius, $C_{\text{ext}}$ is the extinction cross-section for a single particle in $nm^2$, $l$ is the optical path length in nm, $C_{\text{Au}_x\text{Ag}_{x-1}}$ is the concentration of the alloy $Au_x Ag_{x-1}$ in $g\,cm^{-3}$, and $f$ is a constant which depends on the average bulk density $\rho$ of the alloy and is given by

$$f = \frac{4\pi\rho}{3}. \tag{2}$$

In Table 1, the concentrations of each of the alloy clusters used for our calculations and the corresponding $f$ values in $g\,cm^{-3}$ are presented.

TABLE 1: Concentrations, $f$ values, and bulk free-electron gas parameters for Au/Ag alloys of different compositions.

| Molar ratio of Au and Ag | $C_{\mathrm{Au}_x\mathrm{Ag}_{x-1}} \times 10^{-4}$ (g cm$^{-3}$) | $f$ (g cm$^{-3}$) | $v_f \times 10^6$ (m s$^{-1}$) | $\omega_d \times 10^{13}$ (s$^{-1}$) | $\omega_p \times 10^{16}$ (s$^{-1}$) |
|---|---|---|---|---|---|
| 1/0 | 2.600 | 186.183 | 1.390 | 3.225 | 1.350 |
| 9/1 | 2.482 | 177.684 | 1.390 | 3.170 | 1.352 |
| 3/1 | 2.306 | 164.936 | 1.390 | 3.086 | 1.355 |
| 1/1 | 2.012 | 143.689 | 1.390 | 2.948 | 1.360 |
| 1/3 | 1.718 | 122.442 | 1.390 | 2.809 | 1.365 |
| 1/9 | 1.541 | 109.694 | 1.390 | 2.726 | 1.368 |
| 0/1 | 1.424 | 101.195 | 1.390 | 2.670 | 1.370 |

The extinction cross-section of spherical particles embedded in a medium of refractive index $N$ can be calculated by

$$C_{\mathrm{ext}} = 2\frac{\pi}{k^2} \sum_{n=1}^{\infty} (2n+1) \Re(a_n + b_n), \qquad (3)$$

where $k = 2\pi N/\lambda$, and $\Re$ is the real part of the sum of the scattering coefficients $a_n$ and $b_n$ which are functions of particle radius and light wavelength $\lambda$ (in terms of the Ricatti-Bessel functions). As the absorption band of noble metal nanoparticles is dominated by the free-electron behavior, the dielectric function can be described well through Drude's model. The magnitudes of the real and imaginary parts of the dielectric function of the particles are affected when the particle size is smaller than the mean free path of the conduction electrons. Considering this size dependence and based on Drude's model, size-dependent dielectric functions such as the damping frequency of the particle $\omega_r$ can be calculated using the relation [38, 39]

$$\omega_r = \omega_d + B \frac{v_f}{r}, \qquad (4)$$

where $v_f$ is the electron speed at the Fermi level (Table 1), $\omega_d$ is the bulk alloy damping constant (Table 1), and $B$ is a theory-dependent factor, close to one [38].

The bulk dielectric function $\varepsilon(\omega) = \varepsilon_1(\omega) + i\varepsilon_2(\omega)$ for bimetallic systems $\mathrm{Au}_x\mathrm{Ag}_{(1-x)}$ can be defined by considering the weighted average for each component:

$$\varepsilon_{\mathrm{av}}(\mathrm{Au}_x\mathrm{Ag}_{(1-x)}) = \varepsilon_{\mathrm{av}}(x, \omega) = x\varepsilon(\mathrm{Au}) + x\varepsilon(\mathrm{Ag}), \qquad (5)$$

where $x$ is the volume fraction of one component. The size-dependent dielectric functions of the alloy nanoclusters can be expressed considering Drude's model as

$$\varepsilon'(\omega, r) = \varepsilon'_{\mathrm{bulk}} + \frac{\omega_p^2}{(\omega^2 + \omega_d^2)} - \frac{\omega_p^2}{(\omega^2 + \omega_r^2)},$$

$$\varepsilon''(\omega, r) = \varepsilon''_{\mathrm{bulk}} + \frac{i\omega_p^2 \omega_r}{[\omega(\omega^2 + \omega_r^2)]} - \frac{i\omega_p^2 \omega_d}{[\omega(\omega^2 + \omega_d^2)]}, \qquad (6)$$

where $\omega$, $\omega_p$, and $\omega_d$ are the light frequency, plasmon frequency of the bimetallic Au-Ag alloy, and bulk alloy damping constant, respectively.

For calculations, a modified Mie program developed by Kreibing and Vollmer [38] and compiled in Fortan 77 was utilized. For this purpose, wavelength-dependent refractive indices of gold and silver [41] were included in the data bank of the MieCalc program [42]. A fixed refractive index value (1.33) [43] of water was used in the calculations. For calculating the optical absorption spectrum of each bimetallic colloid, corresponding experimentally obtained size distribution histogram (Figure 4) was used. First, the whole size distribution histogram was divided into several equal size ranges. For each size range, corresponding average particle size was used for calculation of absorption spectrum. On obtaining the absorption spectrum for each of the size ranges, the final absorption spectrum of the sample was obtained by considering the normalized fraction of particles as the weighted average of the corresponding sectional absorption spectrum. Throughout the calculation, the true metal concentrations of the colloids were considered.

## 3. RESULTS AND DISCUSSION

Nanoparticles of noble metals such as gold and silver in the size scale smaller than wavelengths of visible light strongly scatter and absorb light due to surface plasmon resonance (SPR, collective oscillation of conduction electron induced by incident light). The frequency and intensity of SPR band depend on the size, shape, structure, and composition [38, 39, 44] of the metal nanoparticles. While the techniques like TEM and HREM reveal the exact size and shape of those nanoparticles, optical absorption spectra give a quick and gross idea on their shapes and sizes. In this study, we used TEM, HREM, and HAADF, along with optical absorption spectroscopy to study the size, size distribution, fine structure, and composition homogeneity of bimetallic Au/Ag colloids of different compositions.

Absorption spectra of the bimetallic colloids prepared with higher concentrations of metal ions (first set of metal ion solutions) are presented in Figure 1. The monometallic dispersions of Au and Ag revealed absorption peaks at about 520 and 413 nm, respectively. While the SPR peaks for the bimetallic colloids prepared with Au/Ag = 9/1 and 3/1 appeared at the same position as that of monometallic Au, for the colloids with Au/Ag = 1/3, the SPR peak position appeared around 418 nm, which is very close to the SPR position of monometallic Ag. Appearance of no absorption peak in the case of Au/Ag = 1/9 indicates the formation of neither type of nanoparticles. On the other hand, the SPR peak positions (Figure 1(b)) of the colloidal
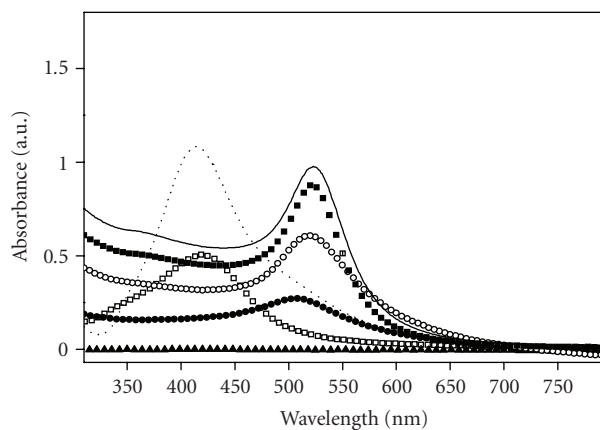
Au/Ag | SPR (nm)
--- | ---
——— Gold | 523
■ 9/1 | 523
○ 3/1 | 520
● 1/1 | 509
□ 1/3 | 421
▲ 1/9 | - - -
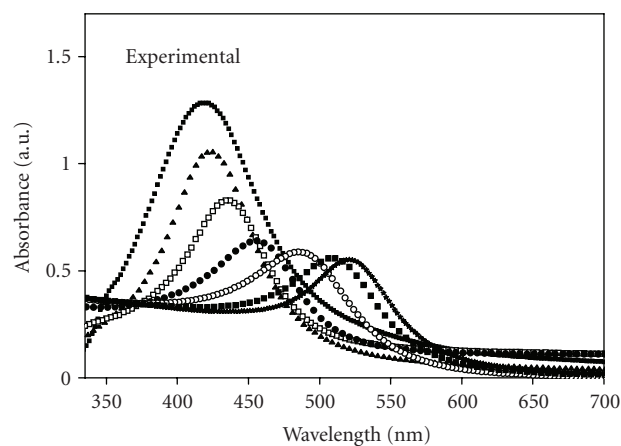·········· Silver | 416

(a)
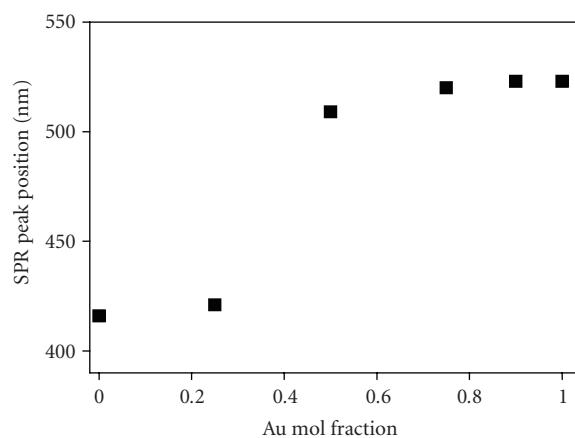


(b)

FIGURE 1: Optical absorption spectra of the bimetallic colloidal samples prepared at different Au/Ag molar ratios, using metal ion solutions of high concentrations (first set of metal ion solutions). The positions of the SPR peaks are plotted against Au mol fraction at the right.

solutions do not obey any linear or quasilinear relationship with the Au mol fraction in the final reaction mixtures. These characteristics demonstrate that with the utilization of metalion concentrations higher than the solubility product ($K_{ps}$) of AgCl$_{(s)}$, it is not possible to obtain Au/Ag alloy nanoparticles.

In Figure 2, the absorption spectra of five bimetallic Au/Ag colloidal dispersions prepared with low concentration of metal ion solutions are presented. For comparison, absorption spectra of monometallic Au and Ag colloids are also presented. The peaks related to the SPR of Au and Ag particles were revealed at about 519 nm and 407 nm, which



Au/Ag | SPR (nm)
--- | ---
★ Gold | 521
■ 9/1 | 509
○ 3/1 | 485
● 1/1 | 457
□ 1/3 | 436
▲ 1/9 | 423
■ Silver | 419

FIGURE 2: Optical absorption spectra of bimetallic colloids prepared with different Au/Ag molar ratios, using low metal ion concentrations (second set of metal ion solutions).

are consistent with the SPR peak positions of gold and silver nanoparticles, respectively [36]. There appeared only one absorption peak for each of the bimetallic colloids. The SPR absorption peaks for the bimetallic colloids are revealed in between the SPR peak positions of monometallic Au and monometallic Ag colloids. Such absorption spectra cannot be obtained either due to the simple physical mixture of monometallic Au and Ag colloidal dispersions, or due to formation of core-shell Au-Ag nanoparticles, where there appear two characteristic absorption peaks [32, 45]. The SPR peak position was blue-shifted in a quasilinear fashion with an increasing Ag content due to the variation of composition of the bimetallic nanoparticles [36]. These observations strongly suggest that each bimetallic particle is a homogeneous Au/Ag alloy one and the novel absorption bands are attributed to the SPR bands of Au-Ag alloy nanoparticles.

In Figure 3, the experimentally obtained SPR peak positions are plotted against the molar ratios of Au and Ag in the reaction mixtures. A quasilinear variation of the SPR peak position with Au mole fraction infers that the composition of the alloy colloids corresponds to the initial concentrations of gold and silver ions in the reaction mixtures. On the other hand, the SPR peak positions of the colloids obtained from their theoretically calculated absorption spectra (presented later) are also presented in Figure 3 (open squares). Close resemblance of the theoretically obtained SPR position values with the corresponding experimentally obtained SPR peak positions indicates that the bimetallic nanoclusters are of true alloy character and of compositions very close to their nominal compositions. A similar variation of SPR peak
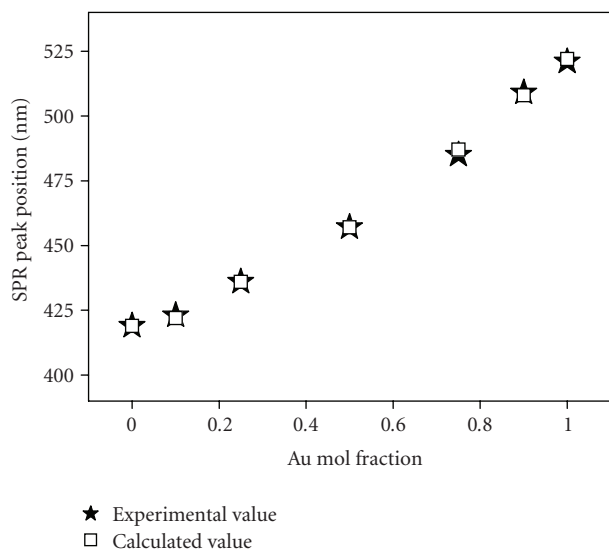
FIGURE 3: Relationship between Au content and surface plasmon resonance peak position of Au/Ag alloy nanoparticles (for the second set of metal ion solutions): (★) experimental and (□) calculated.

position with the variation of Au mole fraction in bimetallic alloy clusters has been observed by Peng et al. [25] for their Au-Ag colloids prepared by laser-assisted synthesis. Therefore, by controlling the initial concentrations of gold and silver ions in the reaction mixtures, we could control the SPR frequency of Au-Ag alloy nanoparticles. It must be noted that the variation of our SPR peak position calculated considering the bulk dielectric constants of Au and Ag is not exactly linear as observed by Link et al. [36] considering the dielectric constant of alloy thin film. However, the variation resembles extremely well the experimentally observed variation. In the further parts of this article, we will discuss only the second batch of samples (prepared with lower concentrations of metal ions in the reaction mixture) for which nanoparticles of uniform composition were obtained.

In order to determine the size of the nanoparticles, TEM analysis has been performed. In Figure 4, typical TEM micrographs of the bimetallic nanoparticles prepared with different molar ratios of Au and Ag (Au/Ag = 9/1, 3/1, 1/1, 1/3, and 1/9) and their respective size distribution histograms are presented. For the histograms, the size of more than 60 particles was measured. The images reveal the formation of nearly spherical nanometric particles. The average particle size varied from 19.4 to 43.2 nm depending on the concentrations of two metals in them. However, the size dispersion decreases with the increase of Au content in them. Absence of bimodal size distribution in the size distribution histograms suggests that the nanoparticles obtained by our synthesis process are not the simple mixture of monometallic particles of Au and Ag. The average particle size increased with the increase of Ag contents in bimetallic nanoparticles until about 75%. Further increase of Ag content reduced the average diameter of the bimetallic nanoparticles. Dependence of particle size on composition

for bimetallic nanoparticles has been studied by several researchers. Esumi et al. [46] and Wu et al. [47] have also observed a positive deviation of mean diameter for Pd/Pt bimetallic nanoparticles on composition.

The increase of particle size on increasing the Ag content in the bimetallic nanoparticles can be explained by considering the reduction velocity of the individual metal ions. As the reduction potential of Ag (0.8 V) is smaller than the reduction potential of Au (1.5 V), the velocity of reduction of Au ions is faster than the velocity of reduction of Ag ions. So, an increasing Ag ion content in the mixture solution inhibits the nucleation rate of the bimetallic nanoparticles, and as a consequence the bimetallic particles grow bigger and dispersed [48].

For a closer observation on the crystallinity, composition, and fine structure of the bimetallic nanoparticles, HREM images of two samples (Au/Ag = 1/1 and 1/3) were recorded. From the HREM images (Figure 5), we can observe the formation of well crystalline multiple twined nanoparticles for both samples. In fact, most of the bimetallic nanoparticles formed in our bimetallic systems were multiple twined. The lattice spacings in the nanoparticles are clearly visible in the amplified images of the selected areas presented as insets. Interplanar spacing calculated for both samples corresponds well with the interplanar spacing of the corresponding alloy structures of fcc phase. However, due to very similar lattice constant values of gold (0.408 nm) and silver (0.409 nm), it was not possible to confirm the alloy nature of the particles with certainty from their HREM images. To confirm the compositional homogeneity of the nanoparticles, we recorded the HAADF images of the alloy particles.

HAADF imaging uses high-angle scattered electrons to obtain spatially resolved images which are able to show suitable details about the compositional inhomogeneity and structural characteristic of bimetallic nanoparticles. High-angle scattering is associated with electron interaction close to the nucleus of the atoms which constitute the sample (Rutherford scattering). So, the scattering phenomenon is strongly dependent on the atomic number (Z). The HAADF image contrast is proportional to the 1.7 power of the average atomic number in the atomic column. As the Z of Ag (47) and Au (79) are amply different, the Z-contrast imaging method should be able to determine the possible inhomogeneity in chemical composition and structural conformation within the bimetallic nanoparticles. Figure 6 shows the typical HAADF images of our bimetallic nanoparticles prepared with Au/Ag = 1/1 and Au/Ag = 1/3 compositions. We can perceive only a homogeneous image contrast for both samples. No significant variation in contrast/intensity over the entire volume of the nanoparticles confirms a homogeneous distribution of metal atoms (Au and Ag) in them. On the contrary, we could have observed HAADF images with inhomogeneous contrasts, as in the case of core-shell nanoparticles [27]. Therefore, the bimetallic nanoparticles obtained under the present synthesis conditions are of homogeneous solid-solution alloys of Au and Ag.

To verify the composition of the nanoparticles, energy dispersive spectroscopy (EDS) analysis on the particles was carried out inside the transmission electron microscope

(a)



(e)



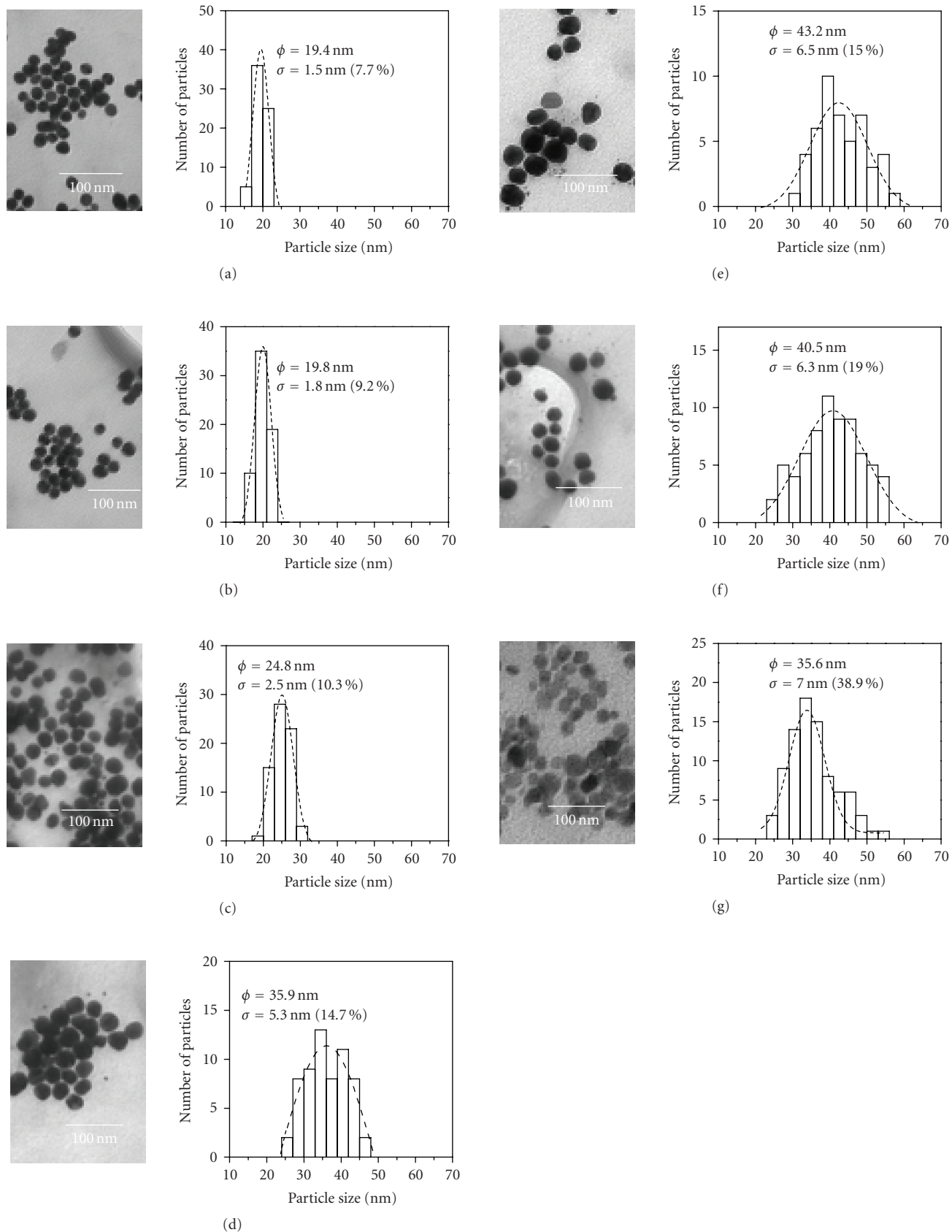(b)



(f)



(c)



(g)



(d)

FIGURE 4: Typical TEM micrographs and corresponding size distribution histograms for the Au/Ag bimetallic nanoparticles (prepared using second set of metal ion solutions) with different molar ratios of Au/Ag: (a) 1/0, (b) 9/1, (c) 3/1, (d) 1/1, (e) 1/3, (f) 1/9, and (g) 0/1. Average particle size $\phi$ and standard deviation $\sigma$ are calculated from the Gaussian fittings of the histograms.
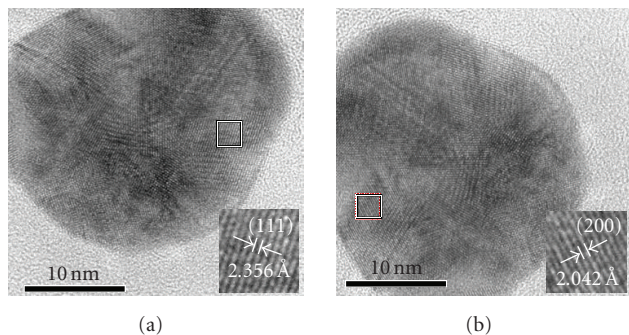
FIGURE 5: High-resolution electron micrographs of bimetallic colloidal particles: (a) Au/Ag = 1/1 and (b) Au/Ag = 1/3 (prepared using second set of metal ion solutions). Amplified images of the marked portions are given as insets.
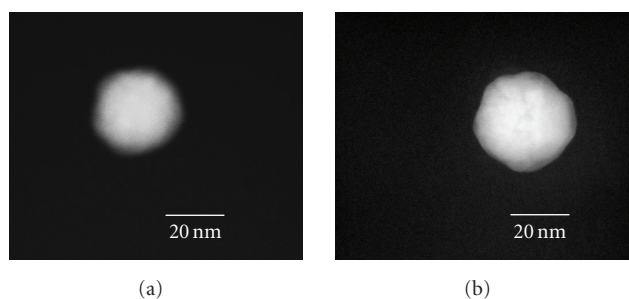


FIGURE 6: Typical HAADF images of (a) Au/Ag (= 1/1) and (b) Au/Ag (= 1/3) bimetallic nanoparticles (prepared using second set of metal ion solutions) showing homogeneous elemental distribution.
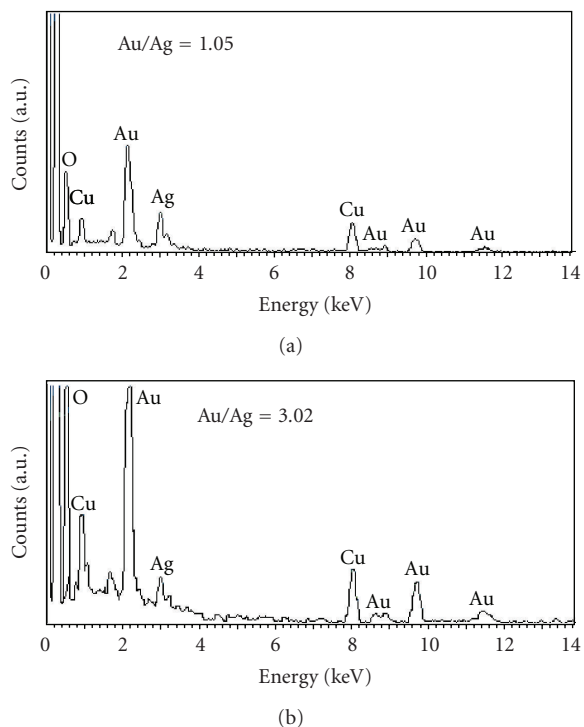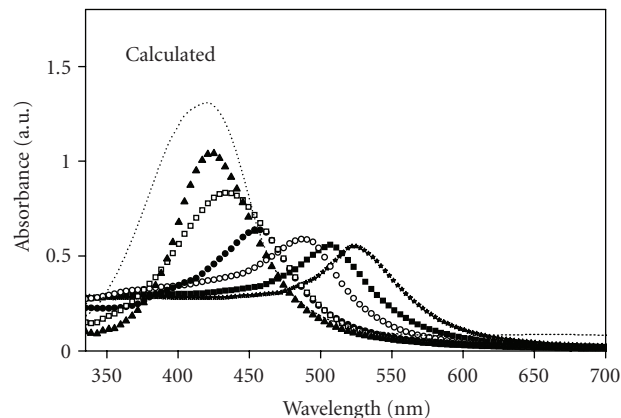


FIGURE 7: EDS spectra of the colloidal samples (prepared with second set of metal ion solutions) with nominal molar ratios: (a) Au/Ag = 1/1 and (b) Au/Ag = 3/1.



| Au/Ag |  | SPR (nm) |
| --- | --- | --- |
| ★ | Gold | 522 |
| ■ | 9/1 | 508 |
| ○ | 3/1 | 487 |
| ● | 1/1 | 457 |
| □ | 1/3 | 436 |
| ▲ | 1/9 | 422 |
| ⋯⋯ | Silver | 419 |

FIGURE 8: Calculated optical absorption spectra for Au-Ag bimetallic colloidal solutions with different molar ratios of Au and Ag.

for three sets of samples with compositions of Au/Ag = 1/1, 1/3, and 1/9. We could not detect any particle of monometallic nature in them. Though the composition of individual particles varied from particle to particle for a given sample, the average composition remained close to its nominal value. The global composition of the samples was also monitored through EDS spectroscopy in a scanning electron microscope. In Figure 7, the EDS spectra of the samples Au/Ag = 1/1 and 3/1 are presented. Along with the Au and Ag emission peaks, there appeared carbon, oxygen, and copper emissions in the EDS spectra of the samples. While the origin of the carbon, oxygen, and copper emissions is related to the carbon film on the grid surface, citrate salt, and copper microgrid, respectively, the obtained Au/Ag atomic ratios for the samples fairly agree with their nominal molar ratios (Au/Ag = 1.05 and 3.02 for the samples preparedwith nominal Au and Ag molar ratios of 1/1 and 3/1, resp.).

Calculated optical absorption spectra of the colloids with different molar ratios of Au and Ag are presented in Figure 8. The shape, intensity, and position of the SPR peak in our calculated absorption spectra were in close resemblance with the corresponding experimentally obtained absorption spectra. The intensity of the SPR peak increases and shifts towards shorter wavelengths with the increase of silver concentration.

## 4. CONCLUSIONS

Au-Ag nanoclusters of solid-solution alloy type could be prepared by simultaneous reduction of gold and silver ions using sodium citrate as reductor. For obtaining bimetallic

clusters of true alloy type while using HAuCl$_4$ and AgNO$_3$ as precursors, the solubility product of the metal ion solutions should be kept below the solubility product (K$_{ps}$) of solid AgCl$_{(s)}$. On the contrary, chlorine ions from HAuCl$_4$ react with silver ions forming solid AgCl, thereby inhibiting the formation of bimetallic alloy clusters. While the composition of the bimetallic alloy clusters could be maintained close to their nominal compositions, the SPR absorption band positions could be tuned precisely close to their theoretical values. Considering true size distribution of the nanoparticles and a modified Mie theory, the optical absorption spectra of the colloids could be reproduced theoretically. Bimetallic Au-Ag alloy nanoparticles of any composition can be prepared using our synthesis method.

## ACKNOWLEDGMENTS

## REFERENCES

[1] J. F. Sánchez-Ramírez, J. L. Jiménez Pérez, A. Cruz Orea, R. Gutierrez Fuentes, A. Bautista-Hernández, and U. Pal, "Thermal diffusivity of nanofluids containing Au/Pd bimetallic nanoparticles of different compositions," *Journal of Nanoscience and Nanotechnology*, vol. 6, no. 3, pp. 685–690, 2006.

[2] R. Esparza, G. Rosas, M. López Fuentes, et al., "Synthesis of gold nanoparticles with different atomistic structural characteristics," *Materials Characterization*, vol. 58, no. 8-9, pp. 694–700, 2007.

[3] J. F. Sánchez-Ramírez, C. Vázquez-López, and U. Pal, "Preparation and optical absorption of colloidal dispersion of Au/Cu nanoparticles," *Superficies y Vacío*, vol. 15, pp. 16–18, 2002.

[4] J. L. Rodríguez-López, J. M. Montejano-Carrizales, U. Pal, et al., "Surface reconstruction and decahedral structure of bimetallic nanoparticles," *Physical Review Letters*, vol. 92, no. 19, Article ID 196102, 4 pages, 2004.

[5] R. Kubo, "Electronic properties of metallic fine particles I," *Journal of Physical Society of Japan*, vol. 17, pp. 975–986, 1962.

[6] M. O. Nutt, K. N. Heck, P. Alvarez, and M. S. Wong, "Improved Pd-on-Au bimetallic nanoparticle catalysts for aqueous-phase trichloroethene hydrodechlorination," *Applied Catalysis B*, vol. 69, no. 1-2, pp. 115–125, 2006.

[7] T. Ishii, H. Otsuka, K. Kataoka, and Y. Nagasaki, "Preparation of functionally PEGylated gold nanoparticles with narrow distribution through autoreduction of auric cation by α-biotinyl-PEG- *block*-[poly(2-(*N*,*N*-dimethylamino)ethyl methacrylate)]," *Langmuir*, vol. 20, no. 3, pp. 561–564, 2004.

[8] A. Sarkar, S. Kapoor, and T. Mukherjee, "Preparation, characterization, and surface modification of silver nanoparticles in formamide," *Journal of Physical Chemistry B*, vol. 109, no. 16, pp. 7698–7704, 2005.

[9] H. Ye and R. M. Crooks, "Effect of elemental composition of PtPd bimetallic nanoparticles containing an average of 180 atoms on the kinetics of the electrochemical oxygen reduction reaction," *Journal of the American Chemical Society*, vol. 129, no. 12, pp. 3627–3633, 2007.

[10] P. Hernández-Fernández, S. Rojas, P. Ocón, et al., "Influence of the preparation route of bimetallic Pt-Au nanoparticle electrocatalysts for the oxygen reduction reaction," *Journal of Physical Chemistry C*, vol. 111, no. 7, pp. 2913–2923, 2007.

[11] A. K. Sharma and B. D. Gupta, "Fibre-optic sensor based on surface plasmon resonance with Ag-Au alloy nanoparticle films," *Nanotechnology*, vol. 17, no. 1, pp. 124–131, 2006.

[12] J.-H. Liu, A.-Q. Wang, Y.-S. Chi, H.-P. Lin, and C.-Y. Mou, "Synergistic effect in an Au-Ag alloy nanocatalyst: CO oxidation," *Journal of Physical Chemistry B*, vol. 109, no. 1, pp. 40–43, 2005.

[13] C. Burda, X. Chen, R. Narayanan, and M. A. El-Sayed, "Chemistry and properties of nanocrystals of different shapes," *Chemical Reviews*, vol. 105, no. 4, pp. 1025–1102, 2005.

[14] S. A. Zynio, A. V. Samoylov, E. R. Surovtseva, V. M. Mirsky, and Y. M. Shirshov, "Bimetallic layers increase sensitivity of affinity sensors based on surface plasmon resonance," *Sensors*, vol. 2, no. 2, pp. 62–70, 2002.

[15] R. Basnayake, Z. Li, S. Katar, et al., "PtRu nanoparticle electrocatalyst with bulk alloy properties prepared through a sonochemical method," *Langmuir*, vol. 22, no. 25, pp. 10446–10450, 2006.

[16] A. M. Molenbroek, S. Haukka, and B. S. Clausen, "Alloying in Cu/Pd nanoparticle catalysts," *Journal of Physical Chemistry B*, vol. 102, no. 52, pp. 10680–10689, 1998.

[17] S.-A. Lee, K.-W. Park, J.-H. Choi, B.-K. Kwon, and Y.-E. Sung, "Nanoparticle synthesis and electrocatalytic activity of Pt alloys for direct methanol fuel cells," *Journal of the Electrochemical Society*, vol. 149, no. 10, pp. A1299–A1304, 2002.

[18] A.-Q. Wang, J.-H. Liu, S. D. Lin, T.-S. Lin, and C.-Y. Mou, "A novel efficient Au-Ag alloy catalyst systemml: preparation, activity, and characterization," *Journal of Catalysis*, vol. 233, no. 1, pp. 186–197, 2005.

[19] R. Esparza, J. A. Ascencio, G. Rosas, J. F. Sánchez-Ramírez, U. Pal, and R. Pérez Campos, "Structure, stability and catalytic activity of chemically synthesized Pt, Au, and Au-Pt nanoparticles," *Journal of Nanoscience and Nanotechnology*, vol. 5, no. 4, pp. 641–647, 2005.

[20] N. K. Chaki, H. Tsunoyama, Y. Negishi, H. Sakurai, and T. Tsukuda, "Effect of Ag-doping on the catalytic activity of polymer-stabilized Au clusters in aerobic oxidation of alcohol," *Journal of Physical Chemistry C*, vol. 111, no. 13, pp. 4885–4888, 2007.

[21] K. Kim, K. L. Kim, and S. J. Lee, "Surface enrichment of Ag atoms in Au/Ag alloy nanoparticles revealed by surface enhanced Raman scattering spectroscopy," *Chemical Physics Letters*, vol. 403, no. 1–3, pp. 77–82, 2005.

[22] Q. Zhang, J. Y. Lee, J. Yang, C. Boothroyd, and J. Zhang, "Size and composition tunable Ag-Au alloy nanoparticles by replacement reactions," *Nanotechnology*, vol. 18, no. 24, Article ID 245605, 8 pages, 2007.

[23] S. Senapati, A. Ahmad, M. I. Khan, M. Sastry, and R. Kumar, "Extracellular biosynthesis of bimetallic Au-Ag alloy nanoparticles," *Small*, vol. 1, no. 5, pp. 517–520, 2005.

[24] P. Raveendran, J. Fu, and S. L. Wallen, "A simple and "green" method for the synthesis of Au, Ag, and Au-Ag alloy nanoparticles," *Green Chemistry*, vol. 8, pp. 34–38, 2006.

[25] Z. Peng, B. Spliethoff, B. Tesche, T. Walther, and K. Kleinermanns, "Laser-assisted synthesis of Au-Ag alloy nanoparticles in solution," *Journal of Physical Chemistry B*, vol. 110, no. 6, pp. 2549–2554, 2006.

[26] B. Karthikeyan, M. Anija, and R. Philip, "*In situ* synthesis and nonlinear optical properties of Au:Ag nanocomposite polymer

films," *Applied Physics Letters*, vol. 88, no. 5, Article ID 053104, 3 pages, 2006.

[27] H. M. Chen, R. S. Liu, L.-Y. Jang, J.-F. Lee, and S. F. Hu, "Characterization of core-shell type and alloy Ag/Au bimetallic clusters by using extended X-ray absorption fine structure spectroscopy," *Chemical Physics Letters*, vol. 421, no. 1–3, pp. 118–123, 2006.

[28] I. Lee, S. W. Han, and K. Kim, "Production of Au-Ag alloy nanoparticles by laser ablation of bulk alloys," *Chemical Communications*, no. 18, pp. 1782–1783, 2001.

[29] H. Takatani, H. Kago, M. Nakanishi, Y. Kobayashi, F. Hori, and R. Oshima, "Characterization of noble metal alloy nanoparticles prepared by ultrasound irradiation," *Reviews on Advanced Materials Science*, vol. 5, no. 3, pp. 232–238, 2003.

[30] A. A. Schmidt and R. Anton, "Anomalous growth behaviour of Pd-Au and Ag-Au alloy particles during vapour deposition on carbon substrates at elevated temperatures," *Surface Science*, vol. 322, no. 1–3, pp. 307–324, 1995.

[31] C. S. Ah, S. D. Hong, and D.-J. Jang, "Preparation of Au$_{core}$Ag$_{shell}$ nanorods and characterization of their surface plasmon resonances," *Journal of Physical Chemistry B*, vol. 105, no. 33, pp. 7871–7873, 2001.

[32] K. Mallik, M. Mandal, N. Pradhan, and T. Pal, "Seed mediated formation of bimetallic nanoparticles by UV irradiation: a photochemical approach for the preparation of "core-shell" type structures," *Nano Letters*, vol. 1, no. 6, pp. 319–322, 2001.

[33] L. Rivas, S. Sánchez-Cortes, J. V. García-Ramos, and G. Morcillo, "Mixed silver/gold colloids: a study of their formation, morphology, and surface-enhanced Raman activity," *Langmuir*, vol. 16, no. 25, pp. 9722–9728, 2000.

[34] S. Mandal, P. R. Selvakannan, R. Pasricha, and M. Sastry, "Keggin ions as UV-switchable reducing agents in the synthesis of Au core-Ag shell nanoparticles," *Journal of the American Chemical Society*, vol. 125, no. 28, pp. 8440–8441, 2003.

[35] L. Lu, H. Wang, Y. Zhou, et al., "Seed-mediated growth of large, monodisperse core-shell gold-silver nanoparticles with Ag-like optical properties," *Chemical Communications*, no. 2, pp. 144–145, 2002.

[36] S. Link, Z. L. Wang, and M. A. El-Sayed, "Alloy formation of gold-silver nanoparticles and the dependence of the plasmon absorption on their composition," *Journal of Physical Chemistry B*, vol. 103, no. 18, pp. 3529–3533, 1999.

[37] Z. Peng, B. Spliethoff, B. Tesche, T. Walther, and K. Kleinermanns, "Laser-assisted synthesis of Au-Ag alloy nanoparticles in solution," *Journal of Physical Chemistry B*, vol. 110, no. 6, pp. 2549–2554, 2006.

[38] U. Kreibing and M. Vollmer, *Optical Properties of Metal Clusters*, vol. 25, Springer, Berlin, Germany, 1995.

[39] C. F. Bohren and D. R. Huffman, *Absorption and Scattering of Light by Small Particles*, Wiley-Interscience, New York, NY, USA, 1998.

[40] P. Mulvaney, "Surface plasmon spectroscopy of nanosized metal particles," *Langmuir*, vol. 12, no. 3, pp. 788–800, 1996.

[41] P. B. Johnson and R. W. Christy, "Optical constants of the noble metals," *Physical Review B*, vol. 6, no. 12, pp. 4370–4379, 1972.

[42] M. Bernhard and L. Eberhard, "MieCalc-freely configurable program for light scattering calculations (Mie theory)," 2006, http://www.lightscattering.de/MieCalc/eindex.html.

[43] R. C. Weast, M. J. Astle, and W. H. Beyer, Eds., *CRC Handbook of Chemistry and Physics*, CRC Press, Boca Raton, Fla, USA, 65th edition, 1984.

[44] M. A. El-Sayed, "Some interesting properties of metals confined in time and nanometer space of different shapes," *Accounts of Chemical Research*, vol. 34, no. 4, pp. 257–264, 2001.

[45] M. Liu and P. Guyot-Sionnest, "Synthesis and optical characterization of Au/Ag core/shell nanorods," *Journal of Physical Chemistry B*, vol. 108, no. 19, pp. 5882–5888, 2004.

[46] K. Esumi, M. Shiratori, H. Ishizuka, T. Tano, K. Torigoe, and K. Meguro, "Preparation of bimetallic Pd-Pt colloids in organic solvent by solvent extraction-reduction," *Langmuir*, vol. 7, no. 3, pp. 457–459, 1991.

[47] M.-L. Wu, D.-H. Chen, and T.-C. Huang, "Preparation of Pd/Pt bimetallic nanoparticles in water/AOT/isooctane microemulsions," *Journal of Colloid and Interface Science*, vol. 243, no. 1, pp. 102–108, 2001.

[48] D.-H. Chen and C.-J. Chen, "Formation and characterization of Au-Ag bimetallic nanoparticles in water-in-oil microemulsions," *Journal of Materials Chemistry*, vol. 12, no. 5, pp. 1557–1562, 2002.